

Sequence-Specific and Stereospecific Assignment of Methyl Groups Using Paramagnetic Lanthanides

Michael John,^{†,§} Christophe Schmitz,[‡] Ah Young Park,[†] Nicholas E. Dixon,^{†,-}
Thomas Huber,[‡] and Gottfried Otting*[†]

Contribution from the Research School of Chemistry, Australian National University, Canberra, ACT 0200, Australia, and School of Molecular and Microbial Sciences and Australian Institute for Bioengineering and Nanotechnology, University of Queensland, Brisbane, QLD 4072, Australia

Received July 9, 2007; E-mail: go@rsc.anu.edu.au

Abstract: Pseudocontact shifts (PCSs) induced by a site-specifically bound paramagnetic lanthanide ion are shown to provide fast access to sequence-specific resonance assignments of methyl groups in proteins of known three-dimensional structure. Stereospecific assignments of Val and Leu methyls are obtained as well as resonance assignments of all other methyls, including Met ϵ CH₃ groups. No prior assignments of the diamagnetic protein are required nor are experiments that transfer magnetization between the methyl groups and the protein backbone. Methyl C₂-exchange experiments were designed to provide convenient access to PCS measurements in situations where a paramagnetic lanthanide is in exchange with a diamagnetic lanthanide. In the absence of exchange, simultaneous ¹³C-HSQC assignments and PCS measurements are delivered by the newly developed program Possum. The approaches are demonstrated with the complex between the N-terminal domain of the subunit ϵ and the subunit θ of the *Escherichia coli* DNA polymerase III.

Introduction

Methyl groups are excellent probes for the study of proteins by NMR spectroscopy because of their favorable relaxation properties and intense ¹H NMR signals. When buried, they report on the packing of side chains in the protein core and thus provide important restraints for protein fold determination.¹ On the protein surface, they can serve as hydrophobic probes of protein–protein^{2,3} and protein–ligand⁴ interactions. Methyl groups have also been established as probes of protein dynamics^{5–11} which, in contrast to amide protons, are inert with regard to solvent exchange.

The resonance assignment of methyl groups in ¹³C labeled proteins is usually achieved by magnetization transfer from sequentially assigned backbone resonances.¹² While this approach works well for proteins up to 30 kDa, it is impeded by fast transverse relaxation for proteins of high molecular weight or for paramagnetic proteins. Recent advances use tailored isotope labeling schemes^{13,14} which are expensive and not generally applicable to any type of methyl group. In particular, the methyl groups of methionine residues are hard to assign since any scalar couplings with the ϵ CH₃ group are small.¹⁵

As a further drawback, experiments that transfer magnetization between methyl groups and backbone resonances usually do not afford stereospecific discrimination between the prochiral methyl groups in Val and Leu residues. In this situation, stereospecific assignments require additional, stereospecifically labeled samples^{16–19} or more complicated NMR experiments that often entail cumbersome data analysis.^{20–24}

[†] Australian National University.

[‡] University of Queensland.

[§] Present address: Georg-August Universität, Institute of Inorganic Chemistry, D-37077 Göttingen, Germany.

⁻ Present address: University of Wollongong, School of Chemistry, Wollongong, NSW 2522, Australia.

- (1) Zwahlen, C.; Gardner, K. H.; Sarma, S. P.; Horita, D. A.; Byrd, R. A.; Kay, L. E. *J. Am. Chem. Soc.* **1998**, *120*, 7617–7625.
- (2) Janin, J.; Miller, S.; Chothia, C. *J. Mol. Biol.* **1988**, *204*, 155–164.
- (3) Gross, J. D.; Gelev, V. M.; Wagner, G. *J. Biomol. NMR* **2003**, *25*, 235–242.
- (4) Hajduk, P. J.; Augeri, D. J.; Mack, J.; Mendoza, R.; Yang, J.; Betz, S. F.; Fesik, S. W. *J. Am. Chem. Soc.* **2000**, *122*, 7898–7904.
- (5) Nicholson, L. K.; Kay, L. E.; Baldisseri, D. M.; Arango, J.; Young, P. E.; Bax, A.; Torchia, D. A. *Biochemistry* **1992**, *31*, 5253–5263.
- (6) Muhandiram, D. R.; Yamazaki, T.; Sykes, B. D.; Kay, L. E. *J. Am. Chem. Soc.* **1995**, *117*, 11536–11544.
- (7) Wand, A. J.; Urbauer, J. L.; McEvoy, R. P.; Bieber, R. J. *Biochemistry* **1996**, *35*, 6116–6125.
- (8) Liu, W.; Zheng, Y.; Cistola, D. P.; Yang, D. *J. Biomol. NMR* **2003**, *27*, 351–364.
- (9) Korzhnev, D. M.; Klobber, K.; Kanelis, V.; Tugarinov, V.; Kay, L. E. *J. Am. Chem. Soc.* **2004**, *126*, 3964–3973.
- (10) Tugarinov, V.; Ollerenshaw, J. E.; Kay, L. E. *J. Am. Chem. Soc.* **2005**, *127*, 8214–8225.
- (11) Tugarinov, V.; Kay, L. E. *ChemBioChem* **2005**, *6*, 1–12.

- (12) Montelione, G. T.; Lyons, B. A.; Emerson, S. D.; Tashiro, M. *J. Am. Chem. Soc.* **1992**, *114*, 10974–10975.
- (13) Tugarinov, V.; Kay, L. E. *J. Am. Chem. Soc.* **2003**, *125*, 5701–5706.
- (14) Tugarinov, V.; Kay, L. E. *J. Am. Chem. Soc.* **2003**, *125*, 13868–13878.
- (15) Bax, A.; Delaglio, F.; Grzesiek, S.; Vuister, G. W. *J. Biomol. NMR* **1994**, *4*, 787–797.
- (16) Senn, H.; Werner, B.; Messerle, B. A.; Weber, C.; Traber, R.; Wüthrich, K. *FEBS Lett.* **1989**, *249*, 113–118.
- (17) Neri, D.; Szyperski, T.; Otting, G.; Senn, H.; Wüthrich, K. *Biochemistry* **1989**, *28*, 7510–7516.
- (18) Ostler, G.; Soteriou, A.; Moody, C. M.; Khan, J. A.; Birdsall, B.; Carr, M. D.; Young, D. W.; Feeney, J. *FEBS Lett.* **1993**, *318*, 177–180.
- (19) Kainosho, M.; Torizawa, T.; Iwashita, Y.; Terauchi, T.; Ono, A. M.; Güntert, P. *Nature* **2006**, *440*, 52–57.
- (20) Züderweg, E. R. P.; Boelens, R.; Kaptein, R. *Biopolymers* **1985**, *24*, 601–611.

In the case where the three-dimensional structure of the protein is known prior to the NMR studies, it would be attractive to use the structure to facilitate the NMR resonance assignments. In favorable situations, structure-based resonance assignments can be achieved from NOE data.²⁵ In addition, structure-based assignments of backbone resonances have been achieved using residual dipolar couplings (RDCs) measured with different alignment media²⁶ or using the combined information from pseudocontact shifts (PCSs), RDCs, paramagnetic relaxation enhancements (PREs), and cross-correlated relaxation (CCR) induced by paramagnetic metal ions.²⁷ The structural interpretation of PCSs has been used earlier to support resonance assignments of ligand residues in heme proteins.²⁸ Recent advances in site-specific attachment of single lanthanide ions to proteins^{29–37} extend this approach to long-range paramagnetic effects, with the possibility of tuning the range of focus by choice of a particular lanthanide.^{27,38,39}

Here we show that the analysis of PCSs induced by lanthanide ions presents a powerful tool for the assignment of methyl resonances, which by reference to the 3D structure of the protein works even in situations when connectivities to the backbone resonances are difficult to establish or the backbone resonance assignment is incomplete. Stereospecific assignments of Val and Leu methyls are obtained as well as the assignments of any other methyl resonances, including those of Met ϵ CH₃ groups. We present two C₂-EXSY experiments for the convenient measurement of PCSs in situations where a paramagnetic lanthanide is in exchange with a diamagnetic lanthanide. In addition, an algorithm was developed to assign the ¹³C-HSQC cross-peaks of methyl groups in the situation where no exchange information is available. The approaches are demonstrated with the 30 kDa complex between the N-terminal exonuclease domain ϵ 186 and the subunit θ of *Escherichia coli* DNA polymerase III. The active site of ϵ 186 binds two divalent ions⁴⁰ that can be replaced by a single Ln³⁺ ion.⁴¹

Experimental Section

Sample Preparation. A cyclized version of ϵ 186, cz- ϵ 186, was designed for enhanced stability of the protein in unrelated crystal-

lographic experiments.⁴² Using an intein-based strategy,⁴³ the N-terminal Ser2 and C-terminal Ala186 of ϵ 186 were linked by the nonapeptide TRESGSIEF (numbered 187–195). Apart from the N- and C-terminal residues that are structurally disordered in ϵ 186,⁴⁰ the amide proton chemical shifts of the linear protein are conserved in cz- ϵ 186 within ± 0.05 ppm, indicating that cyclization does not significantly affect the protein structure. The proteins cz- ϵ 186 and θ were prepared, and used to isolate samples of the cz- ϵ 186/ θ complex, essentially as described previously.⁴⁴ NMR experiments made use of three different samples of complexes of unlabeled θ with isotope-labeled cz- ϵ 186: (i) a uniformly ¹³C/¹⁵N-labeled sample (0.5 mM), (ii) a biosynthetically directed fractional ¹³C-labeled sample prepared from 20% ¹³C-glucose (0.5 mM),^{16,17} and (iii) a sample with ¹³C/¹⁵N-Leu (0.15 mM). Samples of ϵ 186/ θ were dialyzed against NMR buffer (20 mM Tris, pH 7.2, 100 mM NaCl, 0.1 mM dithiothreitol, and 0.08% (w/v) NaN₃ in 90% H₂O/10% D₂O).

Lanthanides (Ln³⁺ = La³⁺ or 1:1 mixtures of La³⁺/Dy³⁺ or La³⁺/Yb³⁺) were added from LnCl₃ stock solutions in the same buffer containing total Ln³⁺ concentrations of 30 mM. The 1:1 mixtures were added in slight molar excess to catalyze the metal ion exchange, resulting in exchange rates of a few s⁻¹.^{45,46} Restoration of the apo-complex was achieved by extensive dialysis against buffer containing 1 mM EDTA followed by dialysis against EDTA-free buffer.

NMR Spectroscopy. All NMR experiments were performed at 25 °C on a Bruker AV 800 MHz NMR spectrometer equipped with a cryogenic TCI probe. Sequence-specific resonance assignments of the methyl groups in the diamagnetic state were established by 3D HNCA and (H)CCH-TOCSY spectra of the uniformly ¹³C/¹⁵N labeled sample complexed with 1 equiv of La³⁺ (cz- ϵ 186/ θ /La³⁺) and by reference to the assignments reported for the linear ϵ 186 protein with Mg²⁺.⁴⁷ Stereospecific assignments of Val and Leu methyl groups were obtained from a constant-time (28 ms) ¹³C-HSQC spectrum recorded of the fractionally ¹³C labeled sample. Where possible, the rotameric states of the side chains of Val and Leu residues in the crystal structure of ϵ 186⁴⁰ were confirmed in solution by a 3D NOESY-¹⁵N-HSQC spectrum (mixing time 60 ms) recorded of the uniformly ¹³C/¹⁵N labeled sample.

Sequence-specific resonance assignments of the methyl groups in the paramagnetic state were established by 2D and 3D methyl C₂-EXSY spectra recorded with the pulse schemes of Figure 1 using a mixing period (τ_m) of 480 ms and spectral widths of 30 ppm (¹³C) and 16 ppm (¹H). The 2D spectra were acquired with 160 × 1024 complex data points and 32 scans in 10 h, while the 3D spectra were acquired with 80 × 64 × 1024 complex points and 4 scans in 40 h. For all spectra, the initial t₁ delay was set to half the increment so that folded paramagnetic peaks could be identified by their inverted sign.⁴⁸

The methyl group assignments obtained with these experiments provided the controls for the assignment methods described below.

Manual Resonance Assignments from PCSs. The PCSs measured from EXSY spectra were used to evaluate the possibility of assigning the methyl peaks by comparison with back-calculated PCSs. PCSs were

- (21) Sattler, M.; Schwalbe, H.; Griesinger, C. *J. Am. Chem. Soc.* **1992**, *114*, 1126–1127.
- (22) Karimi-Nejad, Y.; Schmidt, J. M.; Rüterjans, H.; Schwalbe, H.; Griesinger, C. *Biochemistry* **1994**, *33*, 5481–5492.
- (23) Tugarinov, V.; Kay, L. E. *J. Am. Chem. Soc.* **2004**, *126*, 9827–9836.
- (24) Tang, C.; Iwahara, J.; Clore, G. M. *J. Biomol. NMR* **2005**, *33*, 105–121.
- (25) Grishaev, A.; Llinas, M. *Proc. Natl. Acad. Sci. U.S.A.* **2002**, *99*, 6707–6712.
- (26) Jung, Y.-S.; Zweckstetter, M. *J. Biomol. NMR* **2004**, *30*, 25–35.
- (27) Pintacuda, G.; John, M.; Su, X.-C.; Otting, G. *Acc. Chem. Res.* **2007**, *40*, 206–212.
- (28) Senn, H.; Wüthrich, K. *Quart. Rev. Biophys.* **1985**, *18*, 111–134.
- (29) Ma, C.; Opella, S. J. *J. Magn. Reson.* **2000**, *146*, 381–384.
- (30) Dvoretzky, A.; Gaponenko, V.; Rosevear, P. R. *FEBS Lett.* **2002**, *528*, 189–192.
- (31) Wöhnert, J.; Franz, K. J.; Nitz, M.; Imperiali, B.; Schwalbe, H. *J. Am. Chem. Soc.* **2003**, *125*, 13338–13339.
- (32) Ikegami, T.; Verdier, L.; Sakhaii, P.; Grimme, S.; Pescatore, B.; Fiebig, K. M.; Griesinger, C. *J. Biomol. NMR* **2004**, *29*, 339–349.
- (33) Prudêncio, M.; Rohovec, J.; Peters, J. A.; Tocheva, E.; Boulanger, M. J.; Murphy, M. E. P.; Hupkes, H. J.; Kusters, W.; Impagliazzo, A.; Ubbink, M. *Chem. Eur. J.* **2004**, *10*, 3252–3260.
- (34) Leonov, A.; Voigt, B.; Rodriguez-Castañeda, F.; Sakhaii, P.; Griesinger, C. *Chem. Eur. J.* **2005**, *11*, 3342–3348.
- (35) Haberz, P.; Rodriguez-Castañeda, F.; Junker, J.; Becker, S.; Leonov, A.; Griesinger, C. *Org. Lett.* **2006**, *8*, 1275–1278.
- (36) Rodriguez-Castañeda, F.; Haberz, P.; Leonov, A.; Griesinger, C. *Magn. Reson. Chem.* **2006**, *44*, S10–S16.
- (37) Su, X.-C.; Huber, T.; Dixon, N. E.; Otting, G. *ChemBioChem* **2006**, *7*, 1599–1604.
- (38) Allegrozzi, M.; Bertini, I.; Janik, M. B. L.; Lee, Y.-M.; Liu, G. H.; Luchinat, C. *J. Am. Chem. Soc.* **2000**, *122*, 4154–4161.
- (39) Balayssac, S.; Jiménez, B.; Piccioli, M. *J. Biomol. NMR* **2006**, *34*, 63–73.

- (40) Hamdan, S.; Carr, P. D.; Brown, S. E.; Ollis, D. L.; Dixon, N. E. *Structure* **2002**, *10*, 535–546.
- (41) Pintacuda, G.; Keniry, M.; Huber, T.; Park, A. Y.; Dixon, N. E.; Otting, G. *J. Am. Chem. Soc.* **2004**, *126*, 2963–2970.
- (42) Park, A. Y. Ph.D. Thesis. Australian National University, Australia, 2006.
- (43) Williams, N. K.; Prosselkov, P.; Liepinsh, E.; Line, I.; Sharipo, A.; Littler, D. R.; Curmi, P. M. G.; Otting, G.; Dixon, N. E. *J. Biol. Chem.* **2002**, *277*, 7790–7798.
- (44) Hamdan, S.; Bulloch, E. M.; Thompson, P. R.; Beck, J. L.; Yang, J. Y.; Crowther, J. A.; Lilley, P. E.; Carr, P. D.; Ollis, D. L.; Brown, S. E.; Dixon, N. E. *Biochemistry* **2002**, *41*, 5266–5275.
- (45) John, M.; Headlam, M. J.; Dixon, N. E.; Otting, G. *J. Biomol. NMR* **2007**, *37*, 43–51.
- (46) John, M.; Park, A. Y.; Dixon, N. E.; Otting, G. *J. Am. Chem. Soc.* **2007**, *129*, 462–463.
- (47) DeRose, E. F.; Darden, T.; Harvey, S.; Gabel, S.; Perrino, F. W.; Schaaper, R. M.; London, R. E. *Biochemistry*, **2003**, *42*, 3635–3644.
- (48) Bax, A.; Ikura, M.; Kay, L. E.; Zhu, G. *J. Magn. Reson.* **1991**, *91*, 174–178.

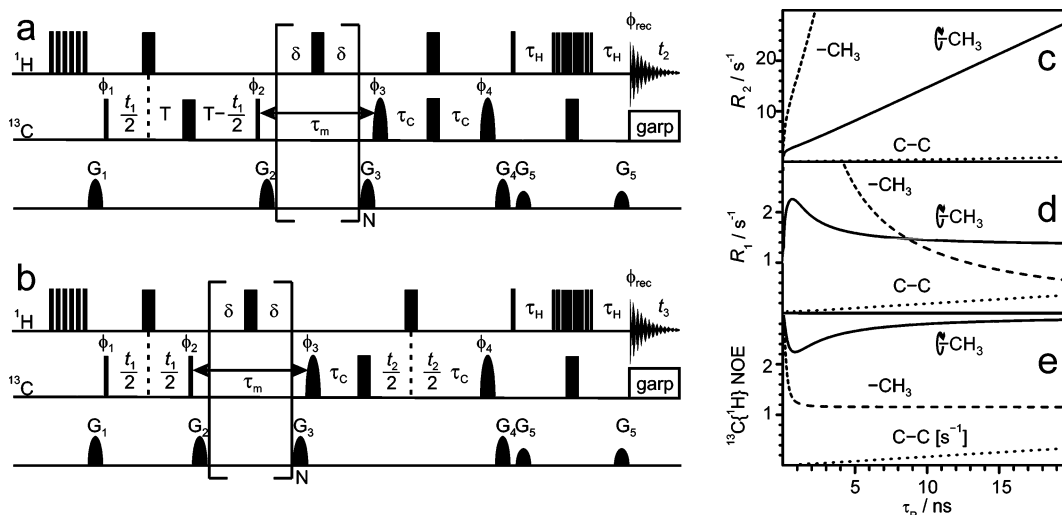


Figure 1. Methyl C_γ-EXSY experiments. (a, b) Pulse schemes of the 2D and 3D versions, respectively. Narrow and wide bars represent radio frequency pulses with flip angles of 90° and 180°, respectively, applied with phase x unless indicated otherwise. Selective ¹³C pulses were applied as a 1.5 ms Q5 pulse prior to the delay τ_c and as a 1.5 ms time-reversed Q5 pulse prior to the delay τ_H , generating an excitation bandwidth of 20 ppm. ¹H saturation is achieved with 120° pulses applied every 5 ms, and the 3-9-19 sequence is used for water suppression. During τ_m , 180°(¹H) pulses are applied every 6 ms with a MLEV-16 supercycle to suppress cross relaxation between ¹H and ¹³C spins. The phase cycle was $\phi_1(x, -x)$, $\phi_2(2x, 2(-x))$, $\phi_3(x)$, $\phi_4(4y, 4(-y))$ and $\phi_{rec}(x, 2(-x), x, -x, 2x, -x)$. States-TPPI was applied to ϕ_1 and ϕ_3 for quadrature detection. Delays: $T = 28$ ms, $\delta = 3$ ms, $\tau_c = 0.75$ ms, $\tau_H = 1.7$ ms. Gradients (G_i) were applied along the z -axis with strengths of 23.2, 14.5, 20.3, 17.5 and 11.6 G/cm. (c–e) Simulated dipolar ¹³C relaxation rates and NOE in isolated CH₃ groups versus molecular rotational correlation time (τ_R) using eqs 1–4 in ref 5: (c) transverse relaxation rate R_2 , (d) longitudinal relaxation rate R_1 , and (e) steady-state ¹³C{¹H} NOE. The dashed line reports the relaxation rates calculated for a static CH₃ group, whereas the solid line takes into account a rapid rotation around the 3-fold symmetry axis with a correlation time $\tau_r = 25$ ps and assuming tetrahedral geometry ($S^2 = 0.111$, $r_{CH} = 1.10$ Å, $r_{CC} = 1.52$ Å).⁷ The dotted line represents the contribution from a neighboring ¹³C spin to R_2 , R_1 , and cross-relaxation (σ), respectively. The vertical axis of the ¹³C–¹³C cross-relaxation rate in panel e is in s⁻¹. Because of the small contribution of PRE to R_1 ,⁴⁵ the ¹³C{¹H} NOE is similar for paramagnetic and diamagnetic proteins.

back-calculated using a Mathematica (Wolfram Research) script and the crystal structure of $\epsilon 186$ (PDB entry 1J53, ref 40). The $\Delta\chi$ -tensor parameters of Dy³⁺ in complex with $\epsilon 186/\theta$ have been reported previously.⁴⁹ The tensor parameters for Yb³⁺ were determined from ¹⁵N-HSQC spectra using the program Echidna⁴⁹ as $\Delta\chi_{ax} = -6.52 \times 10^{-32}$ m³, $\Delta\chi_{th} = 1.12 \times 10^{-32}$ m³, $\alpha = 24.4^\circ$, $\beta = 84.5^\circ$, and $\gamma = 299.5^\circ$ (using the zxz convention of Euler-angle rotations). ¹H PCSs of methyl groups were calculated for each of the three methyl protons individually and averaged. This average is largely insensitive to the rotational position of the methyl group. Residual CSA effects owing to paramagnetic alignment⁵⁰ were disregarded since CSA tensors of methyl groups are small.⁸

The Program Possum. The program Possum (paramagnetically orchestrated spectral solver of unassigned methyls) was developed to assign the cross-peaks of methyl groups in correlation spectra recorded with diamagnetic and paramagnetic metal ions by reference to the 3D structure of the protein and independently determined $\Delta\chi$ tensors. The program requires that the amino-acid type is known (e.g., by residue-type selective ¹³C-labeling). Furthermore, it can accept information about methyl cross-peaks belonging to the same residue (“methyl connectivity” data for Ile, Leu, and Val, as provided by HCCH-TOCSY experiments) and stereospecific information (“methyl specificity” data distinguishing between $\gamma 2$ and $\delta 1$ cross-peaks of Ile, $\delta 1$ and $\delta 2$ cross-peaks of Leu and $\gamma 1$ and $\gamma 2$ cross-peaks of Val, as provided by samples produced with biosynthetically directed fractional ¹³C-labeling^{16,17,23} or stereoselective isotope labeling).^{18,19} In the present version of the program, the methyl connectivity information is always assumed to be available for the diamagnetic state.

The program takes as input the ¹H and ¹³C chemical shifts of methyl groups measured in ¹³C-HSQC spectra and the ¹³C chemical shifts of methyl groups that are too close to the paramagnetic center to be directly

observable in ¹H-detected NMR spectra. By comparing the chemical shifts in the diamagnetic and paramagnetic states, Possum attempts to find the resonance assignment with the lowest residual cost $C(l)$ defined by

$$C(l) = \sum_{i,j,k} x_{i,j,k} (c({}^1\text{H}, i, j, k, l) + c({}^{13}\text{C}, i, j, k, l)) \quad (1)$$

with

$$c(S, i, j, k, l) = \left(\frac{[\text{PCS}_{\text{calc}}^S(k, l) - (\text{para}\delta_{\text{exp}}^S(j, l) - \text{dia}\delta_{\text{exp}}^S(i))]^2}{[e(l)]^2 + [\text{para}\delta_{\text{exp}}^S(j, l) - \text{dia}\delta_{\text{exp}}^S(i)]^2} \right) \quad (2)$$

subject to

$$\left. \begin{aligned} \sum_{j=1}^n \sum_{k=1}^n x_{i,j,k} &= 1, \quad \text{for } i = 1, \dots, n \\ \sum_{i=1}^n \sum_{k=1}^n x_{i,j,k} &= 1, \quad \text{for } j = 1, \dots, n \\ \sum_{j=1}^n \sum_{k=1}^n x_{i,j,k} &= 1, \quad \text{for } k = 1, \dots, n \end{aligned} \right\} \quad (3)$$

$$x_{i,j,k} \in \{0, 1\} \quad (4)$$

where $\text{PCS}_{\text{calc}}^S(k, l)$ is the predicted PCS value for the spin S ($S = {}^{13}\text{C}$ or ¹H) of the methyl group in residue k arising from the paramagnetism of the lanthanide l , $\text{para}\delta_{\text{exp}}^S(j, l)$ is the chemical shift of the resonance j in the presence of the lanthanide l for the spin S , and $\text{dia}\delta_{\text{exp}}^S(i)$ is the diamagnetic resonance i for the spin S . The cost function assigns smaller costs for deviations between calculated and observed PCS values when the experimentally observed PCS is large, while the constant $e(l)$ prevents a singularity in the cost function and accounts for the error in measurements when a spin experiences small paramagnetic effects far away from the paramagnetic center. $e(l)$ scales with the magnitude of

(49) Schmitz, C.; John, M.; Park, A. Y.; Dixon, N. E.; Otting, G.; Pintacuda, G.; Huber, T. *J. Biomol. NMR* **2006**, *35*, 79–87.

(50) John, M.; Park, A. Y.; Pintacuda, G.; Dixon, N. E.; Otting, G. *J. Am. Chem. Soc.* **2005**, *127*, 17190–17191.

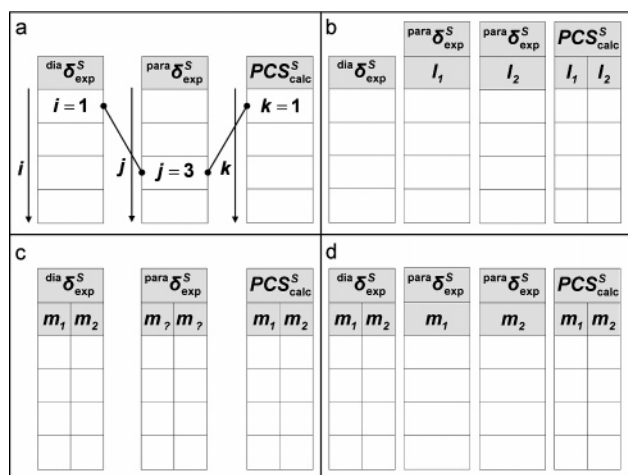


Figure 2. Formulation of the assignment problem depending on the information available. The columns $\text{dia } \delta_{\text{exp}}^S$ and $\text{para } \delta_{\text{exp}}^S$ contain the chemical shifts ($S = {}^{13}\text{C}$ and $S = {}^1\text{H}$ as observed for ${}^{13}\text{C}$ -HSQC cross-peaks) measured in the presence of a diamagnetic or paramagnetic lanthanide, respectively. The column marked $\text{PCS}_{\text{calc}}^S$ contains the ${}^{13}\text{C}$ and ${}^1\text{H}$ PCSs calculated from the $\Delta\chi$ tensor and the 3D structure of the protein. (a) Assignment problem for residues with a single methyl group (Ala, Met, Thr). The indices i and j refer to the cross-peak number in the diamagnetic and paramagnetic state, respectively, and the index k is the residue number in the amino-acid sequence, as in eq 1. The assignment ($i = 1, j = 3, k = 1$) is illustrated by connecting lines. The associated cost can be calculated using eq 2. The other $n - 1$ assignments necessary to calculate the total cost $C(l)$ according to eq 1 are not shown. Overall, this assignment problem is three-dimensional. (b) Simultaneous use of the information from two samples containing the paramagnetic lanthanides l_1 or l_2 creates a four-dimensional assignment problem. (c) For amino acids with two methyl groups (Ile, Leu, Val), the columns $\text{dia } \delta_{\text{exp}}^S$, $\text{para } \delta_{\text{exp}}^S$, and $\text{PCS}_{\text{calc}}^S$ embed the chemical shifts (and PCSs) of two methyl groups (m_1 and m_2). If the methyl-specificity information is not available in the paramagnetic state (illustrated by m_2 in the column $\text{para } \delta_{\text{exp}}^S$), Possum will compute the two possible costs and only keep the lower one. (d) For Ile, Leu, and Val residues, the methyl connectivity information may be available in the diamagnetic state but not in the paramagnetic state. This situation creates a four-dimensional assignment problem for data from a single paramagnetic lanthanide.

the $\Delta\chi$ tensor of the lanthanide l . Empirically determined values ($e(\text{Yb}^{3+}) = 1/6$ ppm and $e(\text{Dy}^{3+}) = 1$ ppm) were used here. Equations 3 and 4 ensure that each calculated PCS and each experimental chemical shift are chosen exactly once within the global assignment.

Equations 1, 3, and 4 present the formulation of the three-index assignment problem⁵¹ which is the three-dimensional instance of the multidimensional assignment problem (MAP). With D being the number of dimensions of the MAP ($D = 3$ in the example above) and n being the size of each of the D sets of data, there are $(n!)^{D-1}$ possible assignments. When D is strictly larger than 2, MAP has been proven to be NP-hard⁵² and, as a result, no algorithm can guarantee the best solution to the problem in a polynomial time. An exhaustive search through the $(n!)^2$ possibilities is impracticable for even the smallest problem sizes. An exact branch and bound algorithm that explores only a part of all possible assignments has been proposed⁵³ and works well for small problem sizes, especially when there is a good agreement between predicted and observed PCS. In the present context, a simulated annealing optimization scheme proved more efficient computationally. The dimensionality D of the assignment problem generated by Possum depends on the residue type, the availability of connectivity information, and the number of different lanthanides used. We have performed calculations with up to 6 dimensions. Examples of 3- and 4-dimensional problems are illustrated in Figure 2.

The program also takes into account the absence of paramagnetic peaks due to PRE by preventing the assignment of observable paramagnetic peaks to methyl groups located closer to the metal ion than a user-specified cutoff. In the present work, cutoffs of 6 and 9 Å were used for the Yb^{3+} and Dy^{3+} complexes, respectively. Paramagnetic peaks missing for any other reason (e.g., spectral overlap) are also tolerated. This is achieved by assigning a cost only to pairings of observable paramagnetic and diamagnetic peaks, whereas a zero cost is associated with any unassigned diamagnetic peak left over. Finally, the program allows for the possibility that paramagnetic shifts may have been observed only for either the ${}^{13}\text{C}$ or the ${}^1\text{H}$ resonance of a methyl group.

The calculation of the assignment starting from the chemical shifts of Table S1 took less than 2 h on an AMD 64 4200+ processor, when using all available information, including methyl connectivity and methyl specificity information and the chemical shifts from the Yb^{3+} and Dy^{3+} complexes. Possum is available upon request.

Results

${}^{13}\text{C}$ -HSQC Spectra of the $\text{cz-}\epsilon 186/\theta/\text{Ln}^{3+}$ Complexes.

Constant-time ${}^{13}\text{C}$ -HSQC spectra of the uniformly ${}^{13}\text{C}$ labeled diamagnetic $\text{cz-}\epsilon 186/\theta/\text{La}^{3+}$ complex and the paramagnetic $\text{cz-}\epsilon 186/\theta/\text{Dy}^{3+}$ and $\text{cz-}\epsilon 186/\theta/\text{Yb}^{3+}$ complexes illustrate the spectral complexity of the methyl region and the effect of the paramagnetism. The spectrum of the $\text{cz-}\epsilon 186/\theta/\text{La}^{3+}$ complex (blue peaks in Figure 3) contains approximately the number of methyl peaks expected for 19 Ala, 14 Thr, 6 Met, 12 Val, 17 Leu, and 14 Ile residues (125 methyl groups). The signals of Met ϵCH_3 groups are particularly well-resolved and easily identified as they appear with opposite sign.

As Dy^{3+} is one of the strongest paramagnetic lanthanide ions,²⁷ the methyl peaks of the $\text{cz-}\epsilon 186/\theta/\text{Dy}^{3+}$ complex (red peaks in Figure 3a) are strongly shifted by PCSs and affected by ${}^1\text{H}$ line broadening due to transverse paramagnetic relaxation enhancement (PRE). Thus, only 55 cross-peaks are observable corresponding to methyl groups with a distance from the Dy^{3+} ion larger than 15 Å, many of them with intensities close to the noise level. Part of the ${}^1\text{H}$ line broadening is caused by unresolved RDCs, including intramethyl RDCs,⁵⁴ originating from the paramagnetically induced alignment of the protein with the magnetic field.

In the $\text{cz-}\epsilon 186/\theta/\text{Yb}^{3+}$ complex, the cutoff distance is reduced to about 9 Å owing to the about 6 times smaller paramagnetic moment of Yb^{3+} so that only 10 methyl peaks are expected to be broadened beyond detection. Of the remaining 115 methyl resonances (red peaks in Figure 3b), only 14 peaks could not be analyzed owing to overlap or very small PCSs at larger distances from the metal ion. Figure 3 shows that for both paramagnetic lanthanides, it is nearly impossible to trace the paramagnetic shift of a ${}^{13}\text{C}$ -HSQC peak using the criterion that the PCSs in the ${}^{13}\text{C}$ and ${}^1\text{H}$ dimensions of the spectrum must be similar. (In methyl groups, the distance between the carbon and the average position of the three protons is less than 0.4 Å.) Therefore, without prior knowledge of resonance assignments, PCS measurements cannot be made manually from ${}^{13}\text{C}$ -HSQC spectra alone.

Methyl C_z -EXSY Experiments. To measure PCS data conveniently and with high sensitivity, we designed an experiment applicable to samples prepared with a 1:1 mixture of paramagnetic and diamagnetic metal ions, where chemical exchange between the metal ions leads to exchange of the

(51) Schell, E. *2nd Symp. Linear Program.* 1955, 615–642.

(52) Karp, R. M. *Complexity of Computer Computations*; Miller, R. E.; Thatcher, J. W., Eds.; Plenum Press: New York, 1972; pp 85–103.

(53) Balas, E.; Saltzman, M. J. *Oper. Res.* **1991**, *39*, 150–161.

(54) Kaikkonen, A.; Otting, G. *J. Am. Chem. Soc.* **2001**, *123*, 1770–1771.

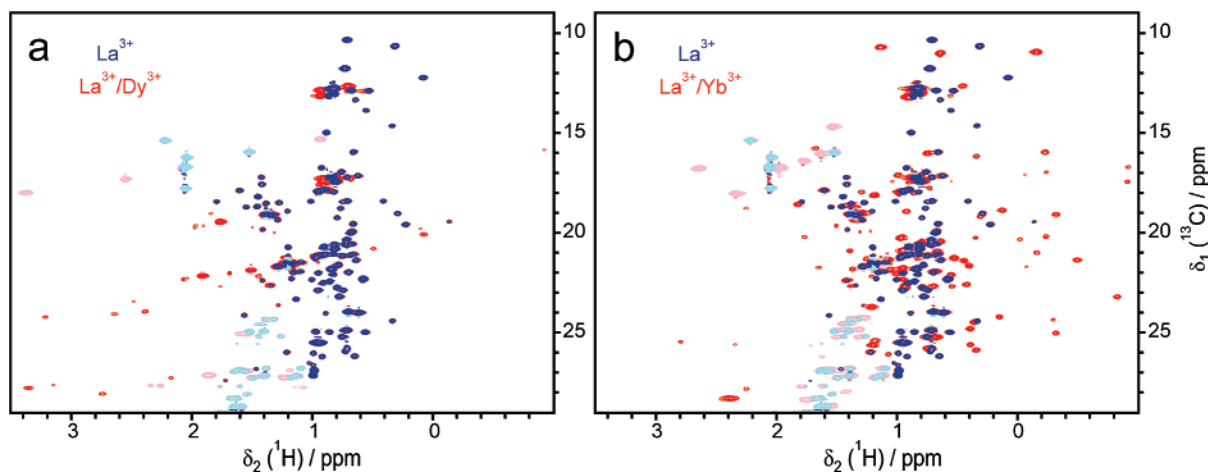


Figure 3. Methyl region of constant-time ^{13}C -HSQC spectra of the *cz*- ϵ 186/ θ complex (containing $^{13}\text{C}/^{15}\text{N}$ labeled *cz*- ϵ 186) in the presence of La^{3+} (blue) and a 1:1 mixture of (a) $\text{La}^{3+}/\text{Dy}^{3+}$ and (b) $\text{La}^{3+}/\text{Yb}^{3+}$ (red). Met ϵCH_3 and CH_2 groups appear with inverted sign (light colors). The spectra were recorded using a constant time of 28 ms and $t_{2\text{max}} = 160$ ms. The spectra of the mixed samples were acquired with 4 times as many scans to compensate for the halving of the effective concentrations.

protein between paramagnetic and diamagnetic states. By generating exchange cross-peaks between methyl peaks of the diamagnetic and paramagnetic lanthanide complexes, the experiment allows the measurement of ^1H and ^{13}C PCS values from a single spectrum. Figure 1 shows 2D and 3D versions of the methyl C_z -EXSY experiment. The pulse sequences are related to previously published N_z -exchange experiments.^{45,55}

During a mixing period τ_m , magnetization is stored as relatively slowly relaxing C_z magnetization. Simulations indicate that, owing to rapid rotation around the 3-fold symmetry axis, longitudinal relaxation rates R_1 of methyl ^{13}C spins are fairly insensitive with respect to molecular size, and barely exceed 2 s^{-1} even for very small proteins (Figure 1d). In the *cz*- ϵ 186/ θ / La^{3+} complex ($\tau_c = 17$ ns), we measured $R_1(^{13}\text{C})$ rates of about 1.6 s^{-1} for the majority of methyl groups. Only a group of highly mobile Thr residues relaxed somewhat faster (2 s^{-1}), whereas the $R_1(^{13}\text{C})$ relaxation in Met ϵCH_3 groups was much slower (about 0.7 s^{-1}). In contrast to transverse relaxation rates R_2 , R_1 rates in macromolecules are barely affected by the paramagnetism of lanthanides.⁴⁵

The experiment yields autopeaks for the diamagnetic and paramagnetic states (dd and pp peaks, respectively) and exchange peaks arising from magnetization exchange from the paramagnetic to the diamagnetic state and vice versa (pd and dp peaks, respectively).

Since the experiment starts from ^{13}C polarization rather than using an INEPT transfer, pd peaks can be detected even for methyl groups that are strongly affected by ^1H PRE in the paramagnetic state and thus invisible in the ^{13}C -HSQC spectrum. Combined with the dd peaks, this allows ^{13}C PCS measurements that are limited only by the (16-fold smaller) ^{13}C PRE.⁴⁶ As indicated previously¹³ and illustrated by the simulations of Figure 1e, ^{13}C polarization in methyl groups of proteins can be very efficiently enhanced using the $\{^1\text{H}\}^{13}\text{C}$ NOE. This holds irrespective of paramagnetism. We observed an about 2-fold increase in ^{13}C polarization in the *cz*- ϵ 186/ θ / La^{3+} complex using 1 s of ^1H irradiation between subsequent scans.

For improved resolution in the ^{13}C dimension and measurement of small ^{13}C PCSs, the 2D experiment is implemented as

a constant-time experiment in the t_1 dimension. The 3D experiment additionally records the ^{13}C frequency of the protein state after the mixing time. Real-time evolution periods in both indirect dimensions yield superior sensitivity for residues with substantial ^{13}C PRE that commonly also have larger PCSs. Selective ^{13}C pulses select the spectral window of the methyl ^{13}C resonances of the diamagnetic complex to limit the spectral width required in the F_1 dimension.

Resonance Assignment of Met, Ala, and Thr Methyl Groups. Figure 4a shows the spectral region of the Met ϵCH_3 cross-peaks of the 2D methyl C_z -EXSY spectrum, recorded with a sample of *cz*- ϵ 186/ θ containing La^{3+} and Dy^{3+} in a 1:1 ratio. Out of six Met residues, four are observed in the ^{13}C -HSQC spectrum of the *cz*- ϵ 186/ θ / Dy^{3+} complex (the cross-peak of Met178 in the paramagnetic state appears with very weak intensity at $\delta_2(^1\text{H}) = 5.33$ ppm). For these residues, both auto and both exchange peaks become visible in the exchange spectrum, forming a rectangle that allows straightforward identification of dd–pp peak pairs, yielding ^{13}C PCS values of 3.28, 1.31, 0.49, and -0.65 ppm. A fifth residue only yields a pd exchange peak with a ^{13}C PCS value of -3.39 ppm.

The measured PCSs can be compared with values predicted from the known structure of ϵ 186⁴² and the previously determined $\Delta\chi$ tensor of Dy^{3+} (Figure 4b).⁴⁹ Only five Met residues belong to the structured part of the protein with predicted ^{13}C PCS values of 3.74 (Met178), 1.30 (Met137), -0.56 (Met87), -1.68 (Met18), and -2.87 ppm (Met107). Met185 is located in the flexible cyclizing loop of *cz*- ϵ 186 and can be immediately assigned to the very intense and narrow resonance with a ^{13}C PCS of 0.49 ppm, in agreement with the PCS of 0.53 ppm observed for the amide proton of this residue. Met18 is the residue closest to the metal ion ($r_{\text{C-Dy}} = 12.0$ Å) and can be assigned to the methyl group that does not show any exchange peak. As Met18 lines the active site this assignment is independently confirmed by its sensitivity to titration with nucleotides (unpublished results). Met107 is the second closest residue ($r_{\text{C-Dy}} = 14.2$ Å) and displays a pd but no dp exchange peak; the assignment of all other Met residues follows in a straightforward manner from the PCS data.

The data show that it is possible to assign a limited number of methyl groups using PCSs only. The situation is more

(55) Farrow, N. A.; Zhang, O.; Forman-Kay, J. D.; Kay, L. E. *J. Biomol. NMR* **1994**, *4*, 727–734.

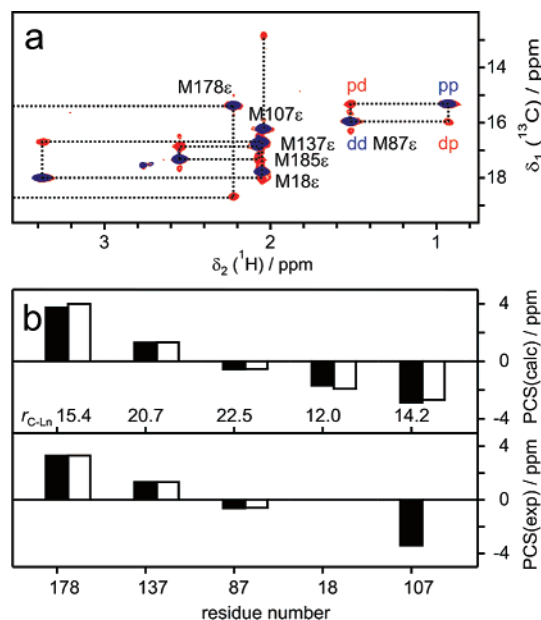


Figure 4. Assignment of Met ϵ CH₃ from PCS. (a) 2D methyl C_α-EXSY spectrum of *cz-ε186/θ* (containing ¹³C/¹⁵N-labeled *cz-ε186*) loaded with a 1:1 mixture of La³⁺ and Dy³⁺ (red), overlaid with the ¹³C-HSQC spectrum (blue). The diamagnetic autopeaks (dd) are labeled with the assignment and connected to the paramagnetic autopeaks (pp) and the exchange peaks (pd and dp) with dashed rectangles. The dp and pp peaks of Met178 are outside the selected spectral region at $\delta_2 = 5.53$ ppm. Met107 only shows a pd exchange peak (vertical dashed line), and neither pp-peak nor exchange peaks are observed for Met18. The spectrum was recorded with a mixing time of 480 ms. (b) Comparison of predicted (top) and measured (bottom) PCSs of Met ϵ CH₃ groups. ¹³C PCS and ¹H PCS values are plotted with filled and open bars, respectively, and sorted according to the predicted ¹³C PCS. The distances r_{C-Ln} are given in Å in the center.

complex for the methyl groups of the other amino acids since with the exception of Ile δ CH₃ groups, the amino acid type cannot be identified from ¹³C-HSQC spectra alone. This information would have to be provided by either the use of residue-specific labeling or additional NMR experiments (in the *cz-ε186/θ/La*³⁺ complex, the amino acid type can readily be identified from a 3D (H)CCH-TOCSY spectrum). In addition, important information is provided by (i) the relative size of ¹³C and ¹H PCS and (ii) whether the paramagnetic ¹H resonance ($r_{C-Dy} > 15$ Å) or only pd exchange peaks ($r_{C-Dy} > 10$ Å, Figures S4 and S5) can be observed.

Assignments of Val, Leu, and Ile Methyl Groups. Val, Leu, and Ile are amino acids with two methyl groups that can easily be linked by correlations observed in TOCSY spectra; combining the PCS data for both methyl groups greatly facilitates the resonance assignment of these residues. This is illustrated in Figure 5 with the *cz-ε186/θ* complex containing 1:1 mixtures of Yb³⁺/La³⁺ (a, b) and Dy³⁺/La³⁺ (c, d), respectively. Whereas a 2D (H)C(C)H-TOCSY experiment (Figure S1, Supporting Information) recorded with short mixing time (12 ms) strongly favors intraresidual methyl-methyl correlations (Figure 5a),⁵⁶ the 2D methyl C_α-EXSY spectrum yields predominantly exchange peaks and only weak $\gamma 1-\gamma 2$ correlations arising from ¹³C-¹³C NOE.⁵⁷ We have also applied the (H)C(C)H-TOCSY experiment to a sample of the pure *cz-ε186/θ/La*³⁺ complex

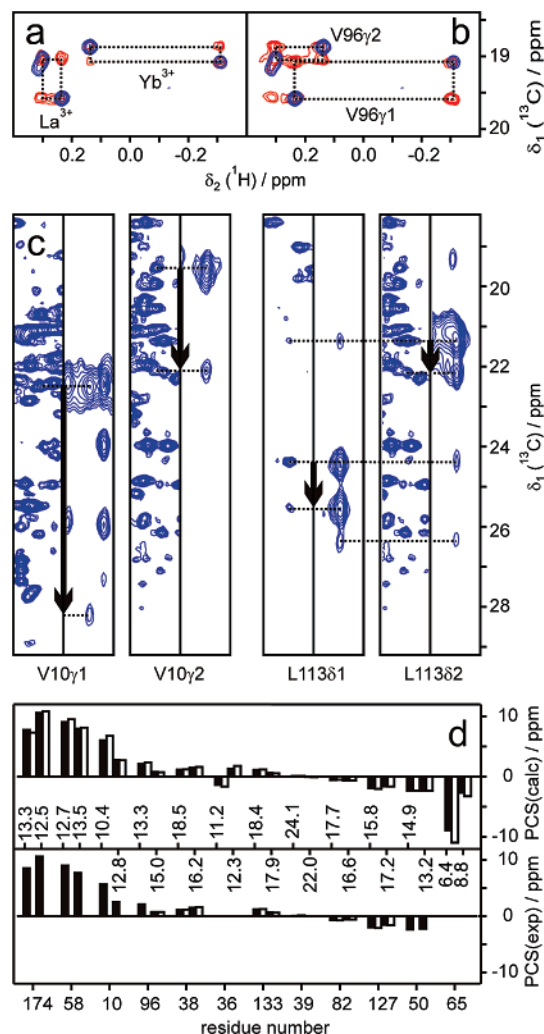


Figure 5. PCS measurements in isopropyl groups of Val and Leu and use of PCSs for stereospecific resonance assignments. (a) Selected spectral region from a 2D (H)C(C)H TOCSY spectrum (red) of *cz-ε186/θ* loaded with a 1:1 mixture of La³⁺ and Yb³⁺, showing the methyl cross-peaks of Val96. The spectrum is overlaid with the ¹³C-HSQC spectrum (blue). Intraresidual correlations between the cross-peaks of the $\gamma 1$ CH₃ and $\gamma 2$ CH₃ groups are identified by dotted lines. The TOCSY spectrum was recorded with 12 ms mixing time. (b) Same spectral region as in panel (a) taken from the 2D methyl C_α-EXSY spectrum of the same sample recorded with a mixing time of 480 ms. (c) Selected strips from the 3D methyl C_α-EXSY spectrum of *cz-ε186/θ* loaded with a 1:1 mixture of La³⁺ and Dy³⁺ (right panels) aligned with corresponding spectral regions from the 2D methyl C_α-EXSY spectrum (left panels). The strips display the methyl group correlations of Val10 and Leu113. The arrows point from the chemical shifts of the diamagnetic auto-peaks (dd) to the chemical shifts of the exchange peaks (pd), indicating the ¹³C PCS. Horizontal lines identify the positions of the dd- and pd-peaks in the δ_1 (¹³C) dimension. The line at 26.35 ppm identifies the ¹³C-¹³C NOEs with the γ CH group of Leu113. (d) Assignment of methyl resonances from the comparison of predicted with experimental PCS. For each Val residue, the distances from the lanthanide in Å are indicated for both methyl carbons in the center of the plot. ¹³C PCS and ¹H PCS values are displayed as filled and open bars, respectively. The residues are sorted according to the predicted ¹³C-PCS, and the PCSs are plotted in the sequence C^{γ1}/H^{γ1}/C^{γ2}/H^{γ2}.

containing selectively ¹³C/¹⁵N-Leu labeled *cz-ε186*, where all $\delta 1-\delta 2$ methyl pairs could be identified (Figure S4, Supporting Information).

Figure 5c compares the measurement of ¹³C PCSs for two residues from strips of 2D and 3D methyl C_α-EXSY spectra. The two experiments are complementary, showing better frequency resolution in the 2D spectrum and generally less cross-

(56) Eaton, H. L.; Fesik, S. W.; Glaser, S. J.; Drobny, G. P. *J. Magn. Reson.* **1990**, *90*, 452–463.

(57) Fischer, M. W. F.; Zeng, L.; Zuiderweg, E. R. P. *J. Am. Chem. Soc.* **1996**, *118*, 12457–12458.

peak overlap in the 3D spectrum. The example of Leu113 shows that one- and two-bond ^{13}C – ^{13}C NOE correlations are visible, but generally of much smaller intensity than the exchange peaks. Through-bond correlations can again be identified from TOCSY spectra. From the combined use of the 2D and 3D C_z -EXSY spectra, all ^{13}C -HSQC cross-peaks observable for any of the methyl groups of the $\text{cz-}\epsilon 186/\theta/\text{Dy}^{3+}$ and $\text{cz-}\epsilon 186/\theta/\text{Yb}^{3+}$ complexes could readily be correlated with the corresponding ^{13}C -HSQC cross-peaks of the $\text{cz-}\epsilon 186/\theta/\text{La}^{3+}$ complex, yielding the PCSs. Compared to the ^{13}C -HSQC spectrum, the methyl C_z -EXSY spectra yielded the ^{13}C chemical shifts in the paramagnetic state for a further 47 methyl groups of the $\text{cz-}\epsilon 186/\theta/\text{Dy}^{3+}$ complex with $r_{\text{C-Dy}}$ distances as short as 10 Å, leaving only 11 methyl groups completely unobservable due to excessive PRE. For the $\text{cz-}\epsilon 186/\theta/\text{Yb}^{3+}$ complex, the methyl C_z -EXSY spectra yielded the ^{13}C chemical shifts for seven additional methyl groups with $r_{\text{C-Yb}}$ distances as short as 6 Å, leaving only one methyl group unobservable.

Figure 5d compares the predicted and measured PCS values for Val methyl groups in the $\text{cz-}\epsilon 186/\theta/\text{Dy}^{3+}$ complex. Each residue is characterized by up to 4 PCS values, resulting in the straightforward assignment of 10 out of 12 residues. Only Val39 did not yield unambiguous PCS data due to resonance overlap, and Val65 is too close to the Dy^{3+} ion. The assignment of Val65 could be made in the $\epsilon 186/\theta/\text{Yb}^{3+}$ complex, where this residue yields large PCS values (Supporting Information). The methyl cross-peaks of Leu residues can be assigned in an analogous way (see below).

Importantly, this approach automatically yields the stereospecific assignment of Val and Leu methyl peaks, as long as different PCSs are observed for the two prochiral methyl groups. Since the methyl carbons in an isopropyl group are separated by 2.5 Å, this is almost always the case (Figure 5d). A rare exception is Val50, where the predicted ^{13}C and ^1H PCSs of the $\gamma 1$ and $\gamma 2$ methyl groups are indistinguishable in both the Dy^{3+} and Yb^{3+} complex.

The methyl groups of Ile residues are particularly easy to assign by PCS, since the spectral ranges of the ^{13}C NMR signals of $\gamma 2$ and $\delta 1$ methyl groups are clearly separated, while intraresidual methyl connectivities can still be obtained from TOCSY spectra.

Automatic Assignments without EXSY Data. C_z -EXSY spectra provide an exceptionally simple way of measuring PCS data. For situations where the metal exchange is too slow for exchange spectra and spectral crowding prevents the straightforward pairing between diamagnetic and paramagnetic ^{13}C -HSQC peaks (Figure 3), we have devised the program Possum which determines the correct peak pairings, their resonance assignments, and their PCS values, using the 3D structure of the protein and the $\Delta\chi$ tensor (that can readily be obtained from, e.g., ^{15}N -HSQC spectra).^{41,49}

The performance of the program was initially tested with simulated data, replacing the experimental paramagnetic shifts of Table S1 by shifts back-calculated from the crystal structure of $\epsilon 186^{40}$ and using as input the crystal structure, the experimental diamagnetic chemical shifts, and the $\Delta\chi$ tensors of Dy^{3+} and Yb^{3+} . In all calculations, it was assumed that the residue types of all methyl resonances were known and the methyl connectivity information of Val, Leu, and Ile residues was available for the diamagnetic state. Except for extreme cases

Table 1. Automatic Assignment of Methyl Groups by the Program Possum^a

residue type	occurrence ^b	La ^c observable	Yb ^d assigned	Dy ^d assigned	La ^e assigned
Met	6 (1)	5	3/5	4/4	3/5
Thr	14 (4)	8	7/7	7/7	7/7
Ala	19 (2)	17	13/13	11/13	14/14
Ile	14 (2)	24	24/24	21/23	24/24
Val	12 (0)	24	20/20	17/20	18/22
Leu	17 (0)	34	34/34	19/25	34/34

^a Obtained using the data reported in Table S1, the crystal structure of $\epsilon 186^{40}$, and $\Delta\chi$ tensors determined from ^{15}N -HSQC spectra as described in the experimental section. The paramagnetic data measured with Yb^{3+} and Dy^{3+} were combined to derive the assignments. ^b Total number of residues in $\text{cz-}\epsilon 186$. The number in brackets refers to residues not observed in the crystal structure; these were excluded from the calculation. ^c Number of methyl groups with coordinates reported in the crystal structure for which cross-peaks were observed in the $\text{cz-}\epsilon 186/\theta/\text{La}^{3+}$ sample. Their unassigned chemical shifts were available for the program. ^d Fraction of correct assignments for the paramagnetic $\text{cz-}\epsilon 186/\theta/\text{Yb}^{3+}$ and $\text{cz-}\epsilon 186/\theta/\text{Dy}^{3+}$ complexes, as indicated. The number in the denominator is the number of methyl groups for which cross-peaks were observed in the presence of Yb^{3+} or Dy^{3+} . ^e Fraction of correct assignments for the diamagnetic $\text{cz-}\epsilon 186/\theta/\text{La}^{3+}$ complex. The number in the denominator is the number of methyl groups for which cross-peaks were observed in at least one of the paramagnetic complexes.

of spectral overlap, the program yielded 100% correct assignments. In a second step, structural uncertainties were simulated by randomly displacing the methyl groups, following a Maxwell–Boltzmann distribution with maxima at 0.35 and 0.7 Å (resulting in maximal atom displacements of 0.75 and 1.5 Å, respectively, always using the same direction of displacement). Even in the case with the maximum structural noise, using only paramagnetic data from the Yb^{3+} complex and neither methyl specificity nor methyl connectivity information in the paramagnetic state, Possum yielded >75% correct assignments of the diamagnetic methyl resonances (Tables S2 and S4). The score increased to >90% when paramagnetic data from the Dy^{3+} complex, methyl specificity information in all complexes, and methyl connectivity information in the Yb^{3+} complex (but not the Dy^{3+} complex) were included (Tables S2 and S3).

The program was subsequently applied to the experimental data of the methyl groups of $\text{cz-}\epsilon 186/\theta$ loaded with La^{3+} , Yb^{3+} , and Dy^{3+} . Table 1 summarizes the results. Using both paramagnetic lanthanides, the assignment is complete and correct for all diamagnetic ^{13}C -HSQC cross-peaks that have observable paramagnetic partners. The only exceptions are swapped assignments for Met18 and Met107 and Val65 and Val82. The first arises from a side-chain conformation that is different in solution than in the single crystal and the second from differences in the predicted and experimental PCSs observed for the peptide segment near Val65.⁴⁶ The assignments of the methyl groups of the Yb^{3+} complex are similarly reliable, whereas the methyl signals of the Dy^{3+} complex are harder to assign (in the absence of methyl connectivity information). Using only data from the Yb^{3+} complex and omitting any methyl specificity information or connectivity information in the paramagnetic state still results in >70% correct assignments of the diamagnetic methyl resonances (Tables S2 and S4).

PCS and Flexibility. Structural differences between the crystal structure of $\epsilon 186$ determined under cryogenic conditions⁴⁰ and the solution structure of the $\text{cz-}\epsilon 186/\theta$ complex become apparent as differences between measured and predicted PCSs. In a few cases, the structural differences interfere with

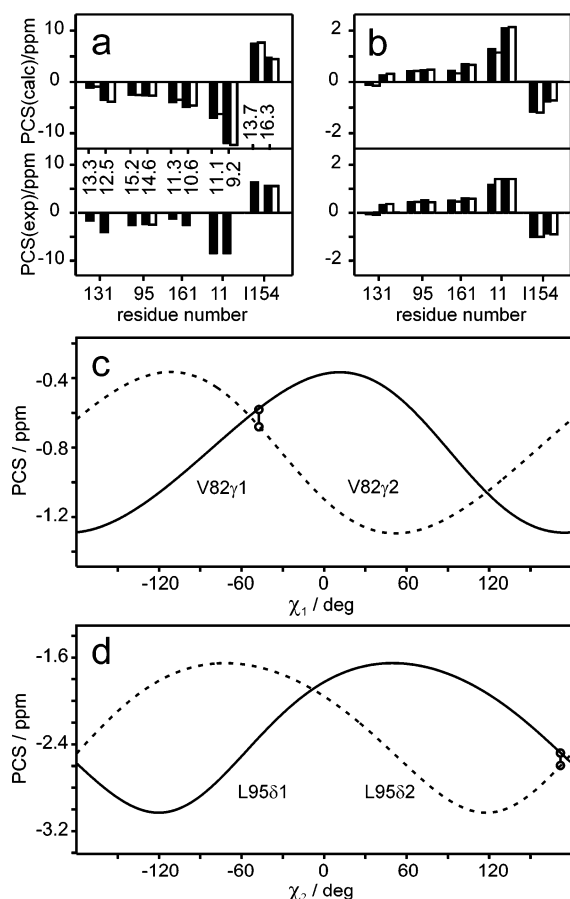


Figure 6. Residues showing deviations between predicted and experimental PCSs. (a) Comparison of calculated and experimental PCS values of Leu131, Leu95, Leu161, Leu11, and Ile154 in the *cz-ε186/θ/Dy³⁺* complex. The data are plotted in the sequence $C^{\gamma 1}/H^{\gamma 1}/C^{\gamma 2}/H^{\gamma 2}$ and $C^{\gamma 2}/H^{\gamma 2}/C^{\delta 1}/H^{\delta 1}$ for the Leu residues and Ile154, respectively. (b) Same as panel a, but for the *cz-ε186/θ/Yb³⁺* complex. (c) Predicted ^{13}C PCSs of the prochiral methyl groups of Val82 in *cz-ε186/θ/Dy³⁺* versus side-chain dihedral angle. The values predicted from the crystal structure of $\epsilon 186^{40}$ are marked. (d) Same as panel c, but for the δCH_3 groups of Leu95.

the resonance assignment. Figure 6a illustrates the situation for the *cz-ε186/θ/Dy³⁺* complex, where the measured PCS values of Leu161 are smaller than predicted and would more closely match the values predicted for Leu131. This can be explained by a small displacement of the peptide segment comprising residues 151–161 that decreases the PCSs of both methyls of Leu161. Smaller PCS values than expected were also observed for the backbone amides of this segment.⁴⁵ The correct assignment would be obtained by focusing on the difference in ^{13}C PCS values between both methyl groups rather than their magnitude (Figure 6a) or by using the data of the *cz-ε186/θ/Yb³⁺* complex which are less strongly distance dependent in the 11 Å distance range (Figure 6b).

In the cases of Val82 and Leu95 in the Dy^{3+} complex, the comparison of experimental and predicted ^{13}C PCS data yields the wrong stereospecific assignment. The χ_1 and χ_2 angles of these residues are -47° and 172° , respectively, in the crystal structure.⁴⁰ Adjusting these angles to -60° and 180° , respectively, inverts the relative size of the ^{13}C PCSs predicted for the two methyl groups, leads to much better agreement between predicted and experimental PCSs, and results in the correct stereospecific assignments (Figure 6c,d). This observation is most simply explained by a small difference between the crystal

and solution structures. Note that the correct assignment could have been obtained for Leu95 in the Yb^{3+} complex (Figure 6b). None of the other Val and Leu residues swapped their stereospecific assignment when we changed their χ_1 angles (χ_2 angles in the case of Leu) by $\pm 10^\circ$.

In the case of Leu11, different NMR criteria suggest that its side chain undergoes dynamic conformational averaging. (i) The ^{13}C PCS values predicted from the structure are -7.0 and -11.9 ppm, whereas the experimental value found for both methyl groups is -8.4 ppm. (ii) In the crystal structure, the two methyl groups are 9.2 and 11.1 Å from the metal ion, but the ^{13}C NMR line widths observed for the methyl groups in the *cz-ε186/θ/Dy³⁺* complex are indistinguishable. (iii) Both methyl resonances overlap with each other in the ^{13}C -HSQC spectrum, indicating similar chemical environments, and their line shapes are narrower than those of most other methyl groups. Remarkably, however, Leu11 is located in the hydrophobic core of the protein and is very well defined in the crystal structure,⁴⁰ although the side chain forms no steric contacts and could access different rotameric states without introducing van der Waals violations with neighboring atoms. Conceivably, the low temperature used in the X-ray experiment may have frozen out a single conformation, whereas a much larger conformational space is accessible at room temperature.

Ile154 presents an example where partial motional averaging may be indicated by a smaller difference observed between the PCSs of the $\delta 1$ and $\gamma 2$ carbon atoms than predicted. The side-chain heavy atoms of this residue shows enhanced B-factors in the crystal structure, in agreement with its location at the protein surface.

Discussion

The present work shows that methyl resonances of ^{13}C -labeled proteins can be assigned solely from PCS data with reference to the 3D structure of the protein, yielding both sequence-specific and stereospecific resonance assignments without having to establish connectivities to backbone resonances. This presents a significant advance over our previous strategy for the assignment of ^{15}N -HSQC spectra, which relied on PCS, PRE, CCR, and RDC data measured on selectively labeled samples.⁴¹

Clearly, any resonance assignment based on comparison of experimental and back-calculated PCS data critically depends on the accuracy of the 3D structure of the protein and is expected to fail for flexible protein segments. Yet, this problem is much less severe than in the case of RDCs,⁵⁸ since PCSs are far less affected by local mobility as long as the nuclear spins are not very close to the paramagnetic center. The robustness of PCSs with regard to structural variations is particularly beneficial for the assignment of Met ϵCH_3 groups that are notoriously difficult to assign by conventional methods. The potential of PCSs for their assignment has been noted previously.⁵⁹

The assignment strategy presented here requires the determination of the $\Delta\chi$ tensor, which can readily be achieved from ^{15}N - ^1H correlation spectra by the Platypus algorithm.⁴¹ Obtaining resonance assignments of methyl groups in this way is attractive because ^{15}N - ^1H correlation spectra of backbone amides and ^{13}C - ^1H correlation spectra of methyl groups can

(58) Sibille, N.; Bersch, B.; Covès, J.; Blackledge, M.; Brutscher, B. *J. Am. Chem. Soc.* **2002**, *124*, 14616–14625.

(59) Bose-Basu, B.; DeRose, E. F.; Kirby, T. W.; Mueller, G. A.; Beard, W. A.; Wilson, S. H.; London, R. E. *Biochemistry* **2004**, *43*, 8911–8922.

be recorded even for high-molecular weight systems.^{60,61} Alternatively, the $\Delta\chi$ -tensor parameters can be determined from assigned diamagnetic NMR resonances and a set of PCSs identified by comparison with the paramagnetic NMR spectrum, either manually or automatically using the Echidna algorithm.⁴⁹ Initial sequence-specific resonance assignments can, if necessary, be achieved by site-directed mutagenesis,^{59,62} for example by mutation of Ile to Val.⁶³

Assignments by PCSs are not limited to metal-binding proteins as different techniques have recently become available that achieve site-specific attachment of lanthanide-tags to proteins devoid of natural metal binding sites.^{29–37} The use of different tags or attachment at different sites readily generates very different $\Delta\chi$ tensors³⁶ that can highlight inconsistencies between experimental and back-calculated PCS values.

If the exchange between paramagnetic and diamagnetic metal ions is too slow to measure exchange spectra, the program Possum can be used to assign the methyl groups in the diamagnetic and paramagnetic state. As expected, the robustness of Possum with regard to small differences between the atomic coordinates of the protein and its actual structure in solution increases with the amount of additional data available. In this respect, data from two paramagnetic metal ions are particularly beneficial, but also information about intraresidual methyl–methyl connectivities or stereospecific identities of methyl groups in Val, Leu, and Ile residues.

The robustness of assignments made by Possum can further be enhanced by the increased spectral resolution afforded by 3D NMR spectra which would greatly facilitate the identification of the corresponding NMR resonances in the diamagnetic and paramagnetic state using the fact that all correlated spins are close in space and therefore experience similar PCSs. For example, 3D (H)CCH-TOCSY or NOESY-¹³C-HSQC spectra would resolve several cross-peaks for each methyl group, which can simultaneously be compared with the 3D structure of the protein and the predicted PCSs to obtain resonance assignments. For methyl groups in the vicinity of the paramagnetic ion, the observation of correlations can be aided by protonless experiments.⁶⁴

Conceivably, assignments by PCS can also be achieved for perdeuterated proteins of increased molecular weight containing selectively protonated methyl groups.⁶⁵ The best spectral resolution in the methyl region of the ¹³C-HSQC spectrum would be obtained for CD₂H groups.¹⁹ Notably, however, the C_z-EXSY experiments described here allowed us to measure all PCS data in the uniformly ¹³C/¹⁵N-labeled and fully protonated sample, that is, the improved spectral resolution of selectively labeled samples was not necessary for our system.

In conclusion, resonance assignments of the ¹³C-HSQC cross-peaks of methyl groups by PCSs induced by a site-specifically attached lanthanide ion present a versatile and convenient technique which can open many opportunities for NMR studies of proteins of known three-dimensional structure. It is anticipated that resonance assignments by this technique will be particularly useful in ligand screening applications.

Acknowledgment. The authors thank Don A. Grundel for source codes of the MAP solver and for useful discussions. M.J. thanks the Humboldt Foundation for a Feodor-Lynen Fellowship. Financial support from the Australian Research Council for project grants, a Federation Fellowship for G.O., and the 800 MHz NMR spectrometer at the ANU is gratefully acknowledged. This work was supported by an award under the Merit Allocation Scheme of the National Facility of the Australian Partnership for Advanced Computing.

Supporting Information Available: Pulse scheme of a (H)C-(C)H-TOCSY experiment for correlations between isopropyl methyl groups, ¹³C-HSQC spectra of uniformly, fractionally, and selectively isotope labeled cz- ϵ 186/ θ , diagrams comparing experimental and predicted PCS values, a table with the chemical shifts of the methyl groups of cz- ϵ 186 observed in the presence of La³⁺, Yb³⁺, or Dy³⁺, and tables reporting the number of methyl groups assigned by Possum. This material is available free of charge via the Internet at <http://pubs.acs.org>.

JA0744753

(60) Fiaux, J.; Bertelsen, E. B.; Horwich, A. L.; Wüthrich, K. *Nature* **2002**, *418*, 207–211.

(61) Sprangers, R.; Kay, L. E. *Nature* **2007**, *445*, 618–622.

(62) Siivari, K.; Zhang, M.; Palmer, A. G.; Vogel, H. J. *FEBS Lett.* **1995**, *366*, 104–108.

(63) Wu, P. S. C.; Ozawa, K.; Lim, S. P.; Vasudevan, S.; Dixon, N. E.; Otting, G. *Angew. Chem., Int. Ed.* **2007**, *47*, 3356–3358.

(64) Bermel, W.; Bertini, I.; Felli, I. C.; Piccioli, M.; Pierattelli, R. *Prog. NMR Spectrosc.* **2006**, *48*, 25–45.

(65) Rosen, M. K.; Gardner, K. H.; Willis, R. C.; Parris, W. E.; Pawson, T.; Kay, L. E. *J. Mol. Biol.* **1996**, *263*, 627–636.